International Refereed Journal of Engineering and Science (IRJES)
ISSN (Online) 2319-183X, (Print) 2319-1821
Volume 7, Issue 2 (February 2018), PP. 16-29

Unsteady Magnetohyrdro Dynamic Convective Heat and Mass Transfer in a Boundary Layer Slip Flow past an Inclined Permeable Surface In The Presence Of Chemical Reaction and Thermal Radiation

Y. Satheesh Kumar Reddy[1], B. Rama Bhupal Reddy[2]
[1]*Research Scholar, Department of Mathematics , Rayalaseema University, Kurnool, A.P.-516003, A.P., India.*
[2]*Professor, Department of Mathematics, K.S.R.M. College of Engineering (Autonomous), Kadapa-516003, A.P., India.*
Corresponding Author: Y. Satheesh Kumar Reddy

ABSTRACT: An analytical study for the problem of mixed convection with chemical reaction and thermal radiation on unsteady magneto hydrodynamics boundary layer flow of viscous, electrically conducting fluid past an inclined permeable surface has been presented. Slip boundary conditions is applied at the porous interface. The non-linear coupled partial differential equations are solved by perturbation technique. The effects of the various parameters on the velocity, temperature, concentration, skin-friction coefficient, rate of heat transfer and rate of mass transfer are discussed in detail.
KEY WORDS: Unsteady, MHD, Slip flow, Thermal radiation and Chemical reaction

---

Date of Submission: 10-02-2018 Date of acceptance: 26-02-2018

I. INTRODUCTION

Mixed convection flows with heat and mass transfer under the influence of a magnetic effect and chemical reaction arise in many transport process both naturally and in many branches of science and engineering applications. They play an important role in many industries like chemical industry, magneto hydrodynamics power generators, power and cooling industry for drying, chemical vapour deposition on surfaces and cooling of nuclear reactors. Such processes occur when the effects of buoyancy forces in forced convection or the effects of forced flow in free convection become significant. Many transport process exist in nature and in industrial applications in which the simultaneous heat and mass transfer occur as a result of combined buoyancy effects of diffusion of chemical species. A few fields of interest in which combined heat and mass transfer plays an important role in design of chemical process in equipment, formation and dispersion of fog, distribution of temperature and moisture over agricultural fields. A theoretical work for both laminar and turbulent mixed convection boundary layer flows has been given in a review paper by Chen and Armaly [1] and in the book by Pop and Ingham [2]. The problem of combined convection under the influence of magnetic field has attracted numerous researchers in view of its applications in geophysics and astrophysics. Soundalgekar et al. [3] analyzed the problem of free convection effects on stokes problem for a vertical plate with transverse applied magnetic field where as Elbasheshy [4] studied MHD heat and mass transfer problem along a vertical plate under the combined buoyancy effects of thermal and species diffusion.

The radiation effect is not considered in the above mentioned studies, when technological processes takes place at high temperatures thermal radiation heat transfer become very important and its effects cannot be neglected. Recent developments in hypersonic flights, missile reentry rocket combustion chambers, gas cooled nuclear reactors and power plants for inter planetary flight, have focused attention of researchers on thermal radiation as a mode of energy transfer, and emphasize the need for inclusion of radiative transfer in these process. The interaction of radiation with mixed convective flows past a vertical plate was investigated by Hossain and Takhar [5]. Aboeldahab [6] studied the radiation effect in heat transfer in an electrically conducting fluid at stretching surface. Heat and mass transfer effects on moving plate in the presence of thermal radiation have been studied by Muthucumarswamy and Kumar Senthil [7] using Laplace technique. Abo-Eldahab and Elgendy [8] presented radiation effect on convective heat transfer in an electrically conducting fluid at a stretching surface with variable viscosity and uniform free stream. Seddeek [9] examined the effect of radiation and variable viscosity on unsteady forced free convection flows in the presence of an align magnetic field. Abdus Satter and Hamid Kalim [10] investigated the unsteady free convection interaction with thermal radiation in a boundary layer flow past a vertical porous plate. Cortell [11] studied the effects of viscous dissipation and

radiation on the thermal boundary layer over a non-linearly stretching sheet. Kim [12] discussed unsteady MHD convective heat transfer past a semi-infinite vertical porous moving plate with variable suction.

Convection in porous media has gained significant attention in recent years because of its importance in engineering applications such as geothermal systems, solid matrix heat exchangers, thermal insulations, oil extraction and store of nuclear waste materials. Convection in also be applied to underground coal gasification, ground water hydrology, iron blast furnaces, wall cooled catalytic reactors, solar power collectors, energy efficient drying processes, cooling of nuclear fuel in shipping flasks, cooling of electronic equipment and natural convection in earth's crust. Reviews of the applications related to convective flows in porous media can be found in Nield and Bejan [13]. The fundamental problem of flow through and past porous media has been studied extensively over the years both theoretically and experimentally [14, 15]. The inadequacy of the no-slip condition is quite evident in polymer melts which often exhibit microscopic wall slip. The boundary conditions to be satisfied at the interface between a porous medium and a fluid layer are the matching of velocity and stresses. Beavers and Joseph [16] were the first to investigate the fluid flow at the interface between a porous medium and fluid layer in an experimental study and proposed a slip boundary conditions at the porous surface. A theoretical justification, using a statistical approach, of the boundary conditions of Beavers and Joseph (BJ) was given by Saffman [17]. The use of Brinkman equation for the porous layer with the continuity of velocity and shear at the interface condition is made. The study in flow past a porous medium is usually based on Darcy's equation with the slip conditions at the interface as proposed by Beavers and Joseph (BJ). Nield [18, 19] applied the Beavers and Joseph (BJ) boundary condition to study the thermal stability of superposed porous and fluid layers for various boundary conditions at the upper and lower of the system. The Beavers-Joseph model has also been used to investigate natural convection within systems of superposed porous and fluid layers. Poulikakos et al. [20] reported a numerical analysis of high Rayleigh convection for the case of a fluid layer on top of porous layer. Rudraiah et al. [21] studied the effect of BJ slip velocity and transverse magnetic field on an electrically conducting viscous fluid in a horizontal channel bounded on both sides by porous substrates of finite thickness which is analogous to the problem of forced convection where the momentum equation is independent of concentration distribution and the diffusion equation is coupled with the velocity distribution using BJ slip condition at the porous interface.

The problem of free convection and mass transfer flow of an electrically conducting fluid past an inclined surface under the influence of a magnetic field has attracted interest in view of its application to geophysics, astrophysics and many engineering problems. Such as cooling of nuclear reactors, the boundary layer control in aerodynamics and cooling towers. In light of these applications, Umemura and Law [22] developed a generalized formulation for the natural convection boundary layer flow over a flat plate with arbitrary inclination. They found that the flow characteristics depend not only on the extent of inclination but also on the distance from the leading edge. Hossain et al. [23] studied the free convection flow from an isothermal plate inclined at a small angle to the horizontal. Anghel et al. [24] presented a numerical solution of free convection flow past an inclined surface. Chen [25] performed an analysis to study the natural convection flow over a permeable inclined surface with variable wall temperature and concentration He observed that increasing the angle of inclination decreases the effect of buoyancy force. Sivasankaran et al. [26] presented a Lie group analysis of natural convection heat and mass transfer in an inclined surface. Bhuvaneswari et al. [27] studied exact analysis of radiation convective flow heat and mass transfer over an inclined plate in a porous medium.

Diffusion rates can be altered tremendously by chemical reactions. The Effect of a chemical reaction depends whether the reaction is homogeneous or heterogeneous. This depends on whether they occur in an interface or as a single phase volume reaction. In a well-mixed system, the reaction is heterogeneous if the reactants are in multiple phases, and homogeneous if the reactants are in the same phase. In most cases of chemical reactions, the reaction rate depends on the concentration of the species itself. Jyothi Bala and Vijaya Kumar [28] analyzed the problem of unsteady MHD heat and mass transfer flow past a semi-infinite vertical porous moving plate with variable suction in the presence of heat generation and homogeneous chemical reaction. Hitesh Kumar [29] presented an analytical solution to the problem of radiative heat and mass transfer over an inclined plate at prescribed heat flux in the presence of chemical reaction. Masthanrao et al. [30] discussed on steady two-dimensional free convection flow of a viscous incompressible electrically conducting fluid through a porous medium bounded by an inclined surface with constant suction velocity, constant heat and mass flux in the presence of uniform magnetic field.

In this paper we have analyzed flow, heat and mass transfer on mixed convection flow of a viscous incompressible electrically conducting fluid over an inclined porous surface in the presence of magnetic field, thermal radiation and chemical reaction using the classical model for the radiative heat flux. Final results are computed for variety of physical parameters which are presented by means of graphs.

II. FORMULATION OF THE PROBLEM

We consider unsteady two dimensional flow of an incompressible, viscous, electrically conducting and heat-absorbing fluid past a semi-infinite inclined permeable surface embedded in a uniform porous medium which is subject to slip boundary condition at the interface of porous and fluid layers. A uniform transverse magnetic field of magnitude B_0 is applied in the presence of radiation and concentration buoyancy effects in the direction of y^* axis. We made the following assumptions

1. The transversely applied magnetic field and magnetic Reynolds number are very small.
2. The induced magnetic field and the Hall effects are neglected.
3. There is no applied voltage which implies the absence of an electric field.
4. The length of the plate is large enough so all the physical variables are independent of x^*.
5. The wall is maintained at constant temperature T_w and concentration C_w higher than the ambient temperature T_∞ and concentration C_∞ respectively.
6. There exists a homogeneous chemical reaction with rate constant D_1 between the diffusing species and the fluid.
7. Porous medium is homogeneous and present everywhere in local thermodynamic equilibrium. Rest of the properties of the fluid and the porous medium are assumed to be constant.

The governing equations for this investigation are based on the balance of mass, linear momentum, energy and concentration species. Taking into consideration these assumptions, the equation that describes the physical situation can be written in Cartesian frame of reference as follows:

Continuity equation:

$$\frac{\partial v^*}{\partial y^*} = 0 \tag{1}$$

Momentum equation:

$$\frac{\partial u^*}{\partial y^*} + \upsilon^* \frac{\partial u^*}{\partial y^*} = -\frac{1}{\rho}\frac{\partial p^*}{\partial x^*} + \nu \frac{\partial^2 u^*}{\partial y^{*2}} - \frac{\sigma B_0^2}{\rho} u^* + g\cos\phi\beta_T (T^* - T_\infty) + g\cos\phi\beta_c (C^* - C_\infty)$$

(2)

Energy equation:

$$\frac{\partial T^*}{\partial t^*} + \upsilon^* \frac{\partial T^*}{\partial y^*} = \frac{k}{\rho c_p}\frac{\partial^2 T^*}{\partial y^{*2}} - \frac{1}{\rho c_p}\frac{\partial q^*}{\partial y^*} - \frac{Q_0}{\rho c_p}(T^* - T_\infty) + Q_1^*(C^* - C_\infty)$$

(3)

Mass Diffusion equation:

$$\frac{\partial C^*}{\partial t^*} + \upsilon^* \frac{\partial C^*}{\partial y^*} = D\frac{\partial^2 C^*}{\partial y^{*2}} - D_1(C^* - C_\infty)$$

(4)

Where x^* and y^* are the dimensionless distances along and perpendicular to the plate, respectively, u^* and v^* are the components of dimensional velocities along x^* and y^* directions respectively, g is the gravitational acceleration, T^* is the dimensional temperature of the fluid near the plate, T_∞ is the free stream dimensional temperature, C^* is the dimensional concentration, C_∞ is the free stream dimensional concentration, β_T and β_c are the thermal and concentration expansion coefficients, respectively, p^* is the pressure, c_p is the specific heat of constant pressure, B_0 is the magnetic field coefficient, μ is viscosity of the fluid, q_r^* is the radiative heat flux, ρ is the density, k is the thermal conductivity, σ is the magnetic permeability of the fluid, $\nu = \frac{\mu}{\rho}$ is the kinematic viscosity, D is the molecular diffusivity, Q_0 is the dimensional heat absorption coefficient, Q_1^* is the coefficient of proportionality of the absorption of the radiation and ϕ is the angle of inclination. The fourth and fifth terms on RHS of the momentum equation (2) denote the thermal and concentration buoyancy effects, respectively. The second and third term on the RHS of equation (3) denote the inclusion of the effect of thermal radiation and heat absorption effects, respectively.

The radiative heat flux is given by $\frac{\partial q^*}{\partial y^*} = 4(T^* - T_\infty)I^*$ (5)

Where $I^* = \int_0^\infty K_{\lambda w} \frac{\partial e_{b\lambda}}{\partial T^*} d\lambda$, where $K_{\lambda w}$ is the absorption coefficient at the wall and $e_{b\lambda}$ is plank's function.

Under these assumptions, the appropriate boundary conditions for velocity involving slip flow, temperature and concentration fields are defined as

$$u^* = u^*_{slip} = \frac{\sqrt{k}}{\alpha}\frac{\partial u^*}{\partial y^*}, \quad T^* = T_w + \in (T_w - T_\infty)e^{n^* t^*}, \quad C^* = C_w + \in (C_w - C_\infty)e^{n^* t^*} \text{ at } y^* = 0$$

$$u^* \to U^*_\infty(1 + \in e^{n^* t^*}), \quad T^* \to T_\infty, \quad C^* \to C_\infty \text{ as } y^* \to \infty \tag{6}$$

Where T_w and C_w are the wall dimensional temperature and concentration respectively, *k* is the permeability of the porous medium and α is the porous parameter. It is clear from equation (1) that the suction velocity at the plate surface is a function of time only. Assuming that, the suction velocity takes the following exponential form:

$$\upsilon^* = -V_0(1 + \in Ae^{n^* t^*}) \tag{7}$$

Where A is a real positive constant, $\in A$ are small less than unity, and V_0 is a scale of suction velocity which has non-zero positive constant. Outside the boundary layer, equation (2) gives

$$-\frac{1}{\rho}\frac{dp^*}{dx^*} = \frac{dU^*_\infty}{dt^*} + \frac{\sigma}{\rho}B_0^2 u^*_\infty \tag{8}$$

Introduce the following non-dimensional quantities

$$u = \frac{u^*}{U_0}, \quad \upsilon = \frac{\upsilon^*}{V_0}, \quad \eta = \frac{V_0 y^*}{\nu}, \quad U_\infty = \frac{U^*_\infty}{U_0}, \quad t = \frac{V_0^2 t^*}{\nu}, \quad \theta = \frac{T^* - T_\infty}{T_w - T_\infty}, \quad C = \frac{C^* - C_\infty}{C_w - C_\infty},$$

$$Sc = \frac{\nu}{D}, \quad n = \frac{n^*\nu}{V_0^2}, \quad Gr = \frac{\beta_T \nu(T_w - T_\infty)}{U_0 V_0^2}, \quad Gm = \frac{\beta_c \nu(C_w - C_\infty)}{U_0 V_0^2}, \quad R = \frac{Q_1^* \nu(C_w - C_\infty)}{V_0^2(T_w - T_\infty)},$$

$$M = \frac{\sigma B_0^2 \nu}{\rho V_0^2}, \quad \Pr = \frac{\mu C_p}{k}, \quad S = \frac{Q_0 \nu}{\rho V_0^2}, \quad F = \frac{4\nu I^*}{\rho V_0^2 C_p}, \quad Kr = \frac{D_1 \nu}{V_0^2} \tag{9}$$

In view of the above non-dimensional variables, the basic field of equations (2)-(4) can be expressed in non-dimensional form as

$$\frac{\partial u}{\partial t} - (1 + \in Ae^{nt})\frac{\partial u}{\partial \eta} = \frac{dU_\infty}{dt} + M(U_\infty - u) + \frac{\partial^2 u}{\partial \eta^2} + Gr_1\theta + Gm_1 C \tag{10}$$

$$\frac{\partial \theta}{\partial t} - (1 + \in Ae^{nt})\frac{\partial \theta}{\partial \eta} = \frac{1}{\Pr}\frac{\partial^2 \theta}{\partial \eta^2} - S\theta + RC - F\theta \tag{11}$$

$$\frac{\partial C}{\partial t} - (1 + \in Ae^{nt})\frac{\partial C}{\partial \eta} = \frac{1}{Sc}\frac{\partial^2 C}{\partial \eta^2} - KrC \tag{12}$$

Where $Gr_1 = Gr\cos\phi$ and $Gm_1 = Gm\cos\phi$. *Gr* is the Grashof number, *Gm* is the solutal Grashof number, Pr is the Prandtl number, *M* is the magnetic field parameter, *F* is the radiation parameter, *Sc* is the Schmidt

number, *S* is the heat source parameter, *Kr* is the chemical reaction parameter and *R* is the absorption of radiation parameter.

The corresponding boundary condition (6) in dimensionless form is

$$u = u_{slip} = k_1 \frac{\partial u}{\partial \eta}, \quad \theta = 1 + \in e^{nt}, \quad C = 1 + \in e^{nt} \text{ at } \eta = 0$$

$$u \to U_\infty = 1 + \in e^{nt}, \quad \theta \to 0, \quad C \to 0 \text{ as } \eta \to \infty \tag{13}$$

Where $k_1 = \frac{\sqrt{k}}{\alpha} \frac{V_0}{\nu}$ is the porous permeability parameter.

III. SOLUTION OF THE PROBLEM

A set of partial differential equations (10)-(12) cannot be solved in closed-form. However, it can be solved analytically after these equations are reduced to a set of ordinary differential equations in dimensionless form which can be done by representing the velocity *u*, temperature θ and concentration C as

$$u = u_0(\eta) + \in e^{nt} u_1(\eta) + O(\in^2)$$

$$\theta = \theta_0(\eta) + \in e^{nt} \theta_1(\eta) + O(\in^2)$$

$$C = C_0(\eta) + \in e^{nt} C_1(\eta) + O(\in^2) \tag{14}$$

Substituting (14) into equations (10)-(12) and equating harmonic and non-harmonic terms, and neglecting the higher order of $O(\in^2)$, and simplifying to get the following pairs of equations for u_0, θ_0, C_0 and u_1, θ_1, C_1.

$$u_0'' + u_0' - Mu_0 = -M - Gr_1\theta_0 - Gm_1 C_0 \tag{15}$$

$$u_1'' + u_1' - (M+n)u_1 = -Au_0' - M - Gr_1\theta_1 - Gm_1 C_1 - n \tag{16}$$

$$\theta_0'' + \Pr\theta_0' - F\Pr\theta_0 = -\Pr S\theta_0 - R\Pr C_0 \tag{17}$$

$$\theta_1'' + \Pr\theta_1' - (F+n+S)\Pr\theta_1 = -\Pr A\theta_0' - R\Pr C_1 \tag{18}$$

$$C_0'' + ScC_0' - KrScC_0 = 0 \tag{19}$$

$$C_1'' + ScC_1' - (Kr+n)ScC_1 = -AScC_0' \tag{20}$$

Where the prime denotes ordinary differentiation with respect to η. The corresponding boundary conditions are

$$u_0 = k_1 u_0', \quad u_1 = k_1 u_1', \quad \theta_0 = 1, \quad \theta_1 = 1, \quad C_0 = 1, \quad C_1 = 1 \quad at \quad \eta = 0$$
$$u_0 = 1, \quad u_1 = 1, \quad \theta_0 = 0, \quad \theta_1 = 0, \quad C_0 = 0, \quad C_1 = 0 \quad at \quad \eta \to \infty \tag{21}$$

Solutions of equations (15) – (20) subject to equation (21) can be shown to be

$$C_0 = e^{-m_1 y} \tag{22}$$

$$C_1 = B_1 e^{-m_1 y} + B_2 e^{-m_2 y} \tag{23}$$

$$\theta_0 = B_3 e^{-m_1 y} + B_4 e^{-m_4 y} \tag{24}$$

$$\theta_1 = B_5 e^{-m_1 y} + B_6 e^{-m_2 y} + B_7 e^{-m_3 y} + B_8 e^{-m_4 y} \tag{25}$$

$$u_0 = 1 + B_9 e^{-m_1 y} + B_{10} e^{-m_3 y} + B_{11} e^{-m_5 y} \tag{26}$$

$$u_1 = 1 + B_{12} e^{-m_1 y} + B_{13} e^{-m_2 y} + B_{14} e^{-m_3 y} + B_{15} e^{-m_4 y} + B_{16} e^{-m_5 y} + B_{17} e^{-m_6 y} \tag{27}$$

Subustituting the above solutions (22) to (27) in (14), we get the final form of velocity, temperature and concentration distribution in the boundary layer as follows:

$$u(\eta,t) = 1 + B_9 e^{-m_1 y} + B_{10} e^{-m_3 y} + B_{11} e^{-m_5 y} + \in e^{nt}(1 + B_{12} e^{-m_1 y} + B_{13} e^{-m_2 y} + B_{14} e^{-m_3 y} + B_{15} e^{-m_4 y} + B_{16} e^{-m_5 y} + B_{17} e^{-m_6 y}) \quad (28)$$

$$\theta(\eta,t) = B_3 e^{-m_1 y} + B_4 e^{-m_4 y} + \in e^{nt}(B_5 e^{-m_1 y} + B_6 e^{-m_2 y} + B_7 e^{-m_3 y} + B_8 e^{-m_4 y}) \quad (29)$$

$$C(\eta,t) = e^{-m_1 y} + \in e^{nt}(B_1 e^{-m_1 y} + B_2 e^{-m_2 y}) \quad (30)$$

The skin-friction coefficient, the Nusselt number and the Sherwood number are important physical parameters for this type of boundary layer flow which are defined and determined as follows:

Skin Friction Coeffieicent:

$$C_f = \left(\frac{\partial u}{\partial \eta}\right)_{\eta=0} = (-m_1 B_9 - m_3 B_{10} - m_5 B_{11}) + \in e^{nt}(-m_1 B_{12} - m_2 B_{13} - m_3 B_{14} - m_4 B_{15} - m_5 B_{16} - m_6 B_{17}) \quad (31)$$

Nusselt Number:

$$Nu = \left(\frac{\partial \theta}{\partial \eta}\right)_{\eta=0} = (-m_1 B_3 - m_3 B_4) + \in e^{nt}(-m_1 B_5 - m_2 B_6 - m_3 B_7 - m_4 B_8) \quad (32)$$

Sherwood number:

$$Sh = \left(\frac{\partial C}{\partial \eta}\right)_{\eta=0} = (-m_1) + \in e^{nt}(-m_1 B_1 - m_2 B_2) \quad (33)$$

IV. RESULTS AND DISCUSSIONS

In this study a numerical analysis is presented to investigate the influence of Ohmic heating and magnetic field on the unsteady combined heat and mass flow of an electrically conducting fluid by mixed convection along a semi-infinite inclined plate taking into account a homogeneous chemical reaction of first order in the presence of thermal radiation. The non-linear coupled governing equations are solved analytically by perturbation technique. Velocity, temperature and concentration profiles are presented graphically analyzed. Final results are computed for variety of physical parameters which are presented by means of graphs. The results are obtained to illustrate the influence of the thermal Grashof number *Gr*, solutal Grasohf number *Gm*, magnetic field parameter *M*, Schmidt number *Sc*, heat absorption parameter *S* , absorption of radiation parameter *R*, chemical reaction parameter *Kr*,radiation parameter F, porous permeability k_1 and angle of inclination ϕ on the velocity, temperature and the concentration profiles, while the values of the physical parameters are taken as constant such as *Pr* = 0.7, *A* =0.5, *n* = 0.1, $\in$ = 0.2, *t* = 1.0, *Gr* = 4.0, *Gm* = 2, *Sc* = 0.6, *S* = 1.0, *R* = 2.0, *M* = 2.0, k_1 = 0.3, S = 2.0, Kr = 0.5, F = 2.0, $\phi = \frac{\pi}{3}$ in all the tables and figures. We have extracted interesting insights regarding the influence of all the parameters that govern this problem. The influence of the parameters *Gr, Gm, Sc, S, M,* k_1, *S, Kr,* F, ϕ and *R* on velocity, temperature and concentration profiles can be analyzed from Figures 1-20.

Figure 1 illustrates the effect of absorption radiation parameter on the velocity in the momentum boundary layer.We note from this figure that there is increase in the velocity profiles with increase in the absorption radiation parameter R.

Figures 2 and 3 show the influence of the thermal buoyancy force parameter *Gr* and solutal buoyancy force parameter *Gm*respectively. As seen from this that maximum peak value attains for Gr or *Gm*= 4.0 and minimum peak value is observed for Gr or *Gm*= 1.0. This is due to the fact that buoyancy force enhances fluid velocity and increase the boundary layer thickness with increase in the value of *Gr* and *Gm*.

The effect of magnetic field on velocity profiles in the boundary layer is depicted in figure 4. From this figure it is seen that the velocity starts from minimum value at the surface and increase till it attains the peak value and then starts decreasing until it reaches to the minimum value at the end of the boundary layer for all the values of magnetic field parameter.

Figure 5 illustrates the effect of radiation on the velocity in the momentum boundary layer, we note from this figure that there is decrease in the velocity profiles with increase in the radiation parameter *F*. The increase of the radiation parameter *F* leads to decrease the boundary layer thickness and to enhance the heat transfer rate in

the presence of thermal and solutal buoyancy force. The effect of chemical reaction parameter *Kr* is highlighted in **figure 6.** The trend of the velocity profiles in this figure is same as those shown in figure 5. From these figures it is observed that the peak value attains near the porous boundary layer.

The effect of increasing the value of the heat absorption parameter S is to decrease the boundary layer as shown in figure 7, which is expected due to the fact that when heat is absorbed the buoyancy force decreases which retards the flow rate and thereby giving rise to decrease in the velocity profiles.

The variation of velocity profile with porous permeability parameter is represented in figure 8. This figure clearly indicates that the value of velocity profile increases with increasing the porous permeability parameter K_1.

We observed from figure 9 that a very low values of Schmidt number, there is increase in the peak velocity near the plate, whereas for higher values of Schmidt number the peak shifts closer to the plate. Further it is observed that the momentum boundary layer decreases with increase in the values of *Sc*.

Figure 10 is a plot of velocity profiles for various values of time in the boundary layer. This figure clearly indicates that the velocity slowly attains the peak value close to the porous boundary after that the profile decreases will it reaches the minimum value as $\eta \to \infty$. This situation is applicable for all time. Further, it is observed that the value of the peak increases with time.

The effect of inclination of the surface on velocity profile is shown in Figure 11. We observe that fluid velocity is decreased for increasing angle ϕ. The fluid has higher velocity when the surface is vertical ($\phi = 0$) than when inclined because of the fact that the buoyancy effect decreases due to gravity components ($g\cos\phi$), as the plate is inclined.

Figure 12 depicts the variation of temperature profile against span wise coordinate η for various values Schmidt number *Sc* for fixed values of other physical parameters. It is observed from this figure that increase in *Sc* decreases temperature distribution throughout the boundary layer due to decrease in boundary layer thickness.

Figure 13 represents graph of temperature distribution with span-wise coordinate η for different values of radiation parameter. From this figure we note that, temperature is very high at the porous boundary and asymptotically decreases to zero as $\eta \to \infty$, satisfying the boundary condition. Further, it is observed from this figure that increase in the radiation parameter decreases the temperature distribution in the thermal boundary layer due to decrease in the thickness of the thermal boundary layer with thermal radiation parameter *F*. This is because large values of radiation parameter correspond to an increase in dominance of conduction over radiation, thereby decreasing the buoyancy force and the thickness of the thermal boundary layer.

Figure 14 has been plotted to depict the variation of temperature profiles against η for different values of heat absorption parameter *S* by fixing other physical parameters. From this figure we observed that temperature $\theta(\eta)$ decreases with increase in the heat absorption parameter *S* because when heat is absorbed, the buoyancy force decreases the temperature profile.

Figure 15 is the graph of temperature profiles $\theta(\eta)$ versus distance η for different values of chemical reaction parameter *Kr*. It can easily be seen that the thermal boundary layer releases the energy which causes the temperature of the fluid to decrease with increase in the chemical reaction parameter *Kr*.

Figure 16 depicts the graph of temperature profile $\theta(\eta)$ for various values of absorption radiation parameter R in the boundary layer. It is seen that the effect of absorption of radiation parameter is to increase temperature in the boundary layer as the radiated heat is absorbed by the fluid which is responsible for increase in the temperature of the fluid very close to the porous boundary layer and its effect diminished far away from the porous boundary.

Figure 17 is drawn for temperature profile $\theta(\eta)$ versus η from the sheet, for different values of time. By analyzing the graph it reveals that temperature increases as time increase in the flow region. This is due to the fact that heat energy is stored in the liquid as time increases.

The effect of chemical reaction rate parameter *Kr* on the species concentration profiles for generative chemical reaction is shown in figure 18. It is noticed for the graph that there is marked effect of increasing the value of the chemical reaction rate parameter *Kr* which is greater than 1 at the start of the boundary layer decreases slowly till it attains the minimum value of zero at the end of the boundary layer and this trend is seen for all the values of reaction rate parameter. Further, it is observed that increasing the value of the chemical reaction decreases the concentration of species in the boundary layer, this is due to the fact that destructive chemical reduces the solutal boundary layer thickness and increases the mass transfer.

Figure 18 shows the effect of Schmidt number *Sc* on concentration profiles. From this figure it is noticed that as increase in the Schmidt number *Sc* decreases the concentration boundary layer thickness which is associated with the reduction in the concentration profiles. Physically, the increase of *Sc* means decrease of molecular

diffusion D. Hence, the concentration of the species is higher for small values of *Sc* and lower for larger values of *Sc*.

Figure 20 is a plot of concentration profiles against η for various values of time *t*. As seen from this plot that concentration of species increases with time in the solutal boundary layer which results in increase in the solutal boundary layer thickness.

Tables 1 shows the effects of porous permeability parameter K_1, radiation parameter *F*, Schmidt number *Sc*, chemical reaction parameter *Kr*, heat absorption parameter *S*, radiation absorption parameter *R*, thermal Grashof number *Gr*, solutal Grashof number *Gm* and angle of inclination ϕ on skin-friction coefficient. From this table it is seen that the effect of K_1, *F*, *Sc*, *Kr*,*S* and ϕ is to decrease skin-friction coefficient C_f whereas effect of *R*, *Gr* and *Gm*is to increase C_f .

Table 2 shows the effects of radiation parameter *F*, Schmidt number *Sc*, chemical reaction parameter *Kr*, heat absorption parameter *S* and radiation absorption parameter *R* on Nusselt number *Nu*. From this table it is noticed that the effect of *F*, *Sc*, *S* and *Kr* is to decrease Nusselt number *Nu* whereas reverse phenomenon is observed in the case of R.

Table 3 shows the effect of Schmidt number *Sc* and chemical reaction parameter *Kr* on Sherwood number *Sh*. It is found from table 3 that Sherwood number decreases with increase in chemical reaction parameter *Kr* or Schmidt number *Sc*.

In order to verify the accuracy of the present results, we have considered the analytical solutions obtained by Kim [12] and computed the numerical results for skin-friction coefficient and local Nusselt number. These computed results are tabulated in Table 4. It is interesting to observe from this table 4 that the present results are in very good agreement with the computed results obtained from analytical solutions of Kim [12], which clearly shows the correctness of the present analytical solutions and computed results.

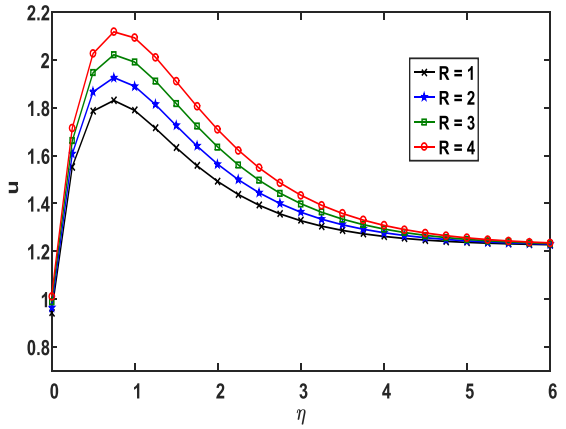

Figure 1: Velocity profiles against span wise co-ordinate η for different values of absorption radiation parameter R

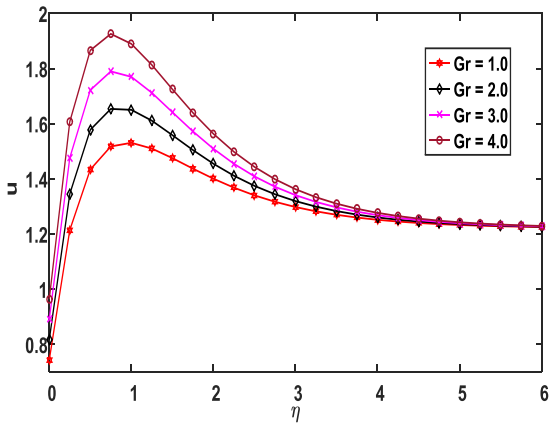

Figure 2: Velocity profiles against span wise co-ordinate η for different values of thermal Grashof number Gr

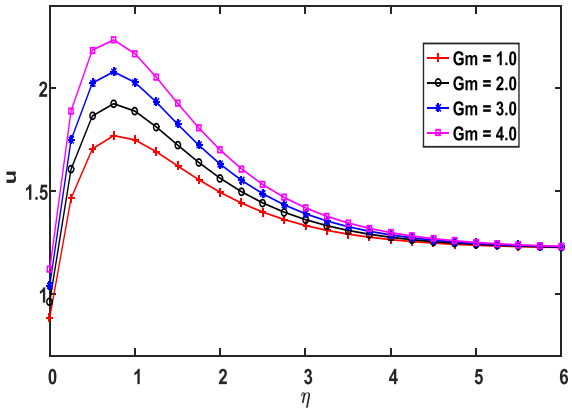

Figure 3: Velocity profiles against span wise co-

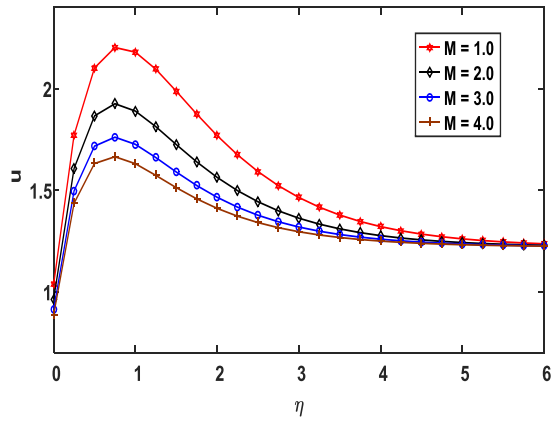

Figure 4: Velocity profiles against span wise co-

ordinate η for different values of solutal Grashof number Gm

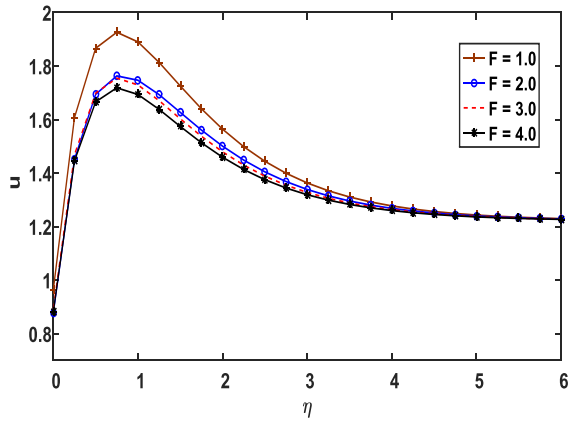

Figure 5: Velocity profiles against span wise co-ordinate η for different values of radiation parameter F

ordinate η for different values of magnetic parameter M

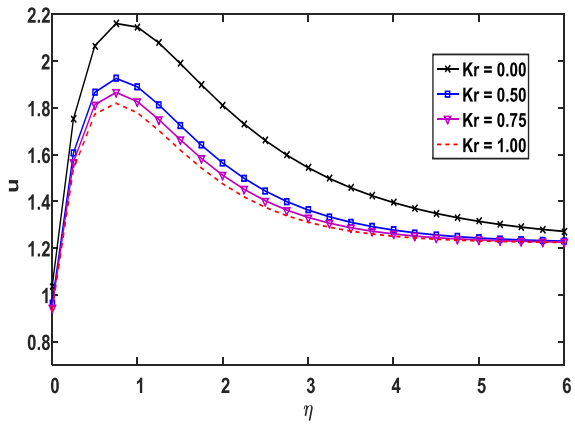

Figure 6: Velocity profiles against span wise co-ordinate η for different values of chemical reaction parameter Kr

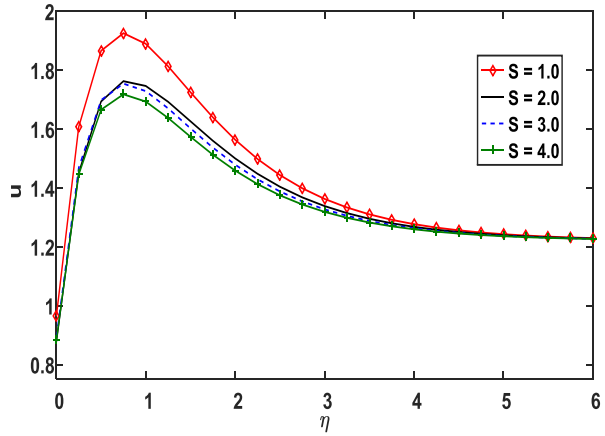

Figure 7: Velocity profiles against span wise co-ordinate η for different values of heat absorption parameter S

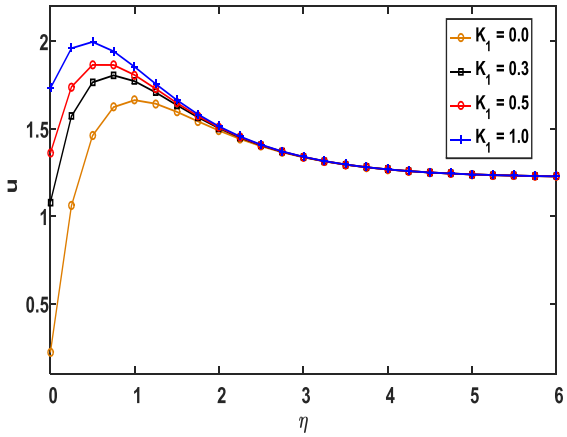

Figure 8: Velocity profiles against span wise co-ordinate η for different values of porous parameter K_1

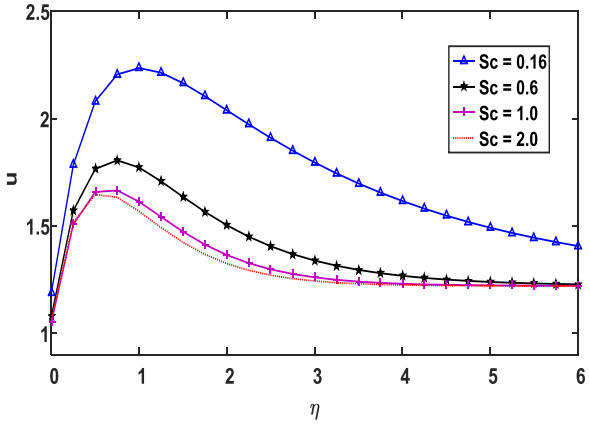

Figure 9: Velocity profiles against span wise co-ordinate η for different values of Schmidt number Sc

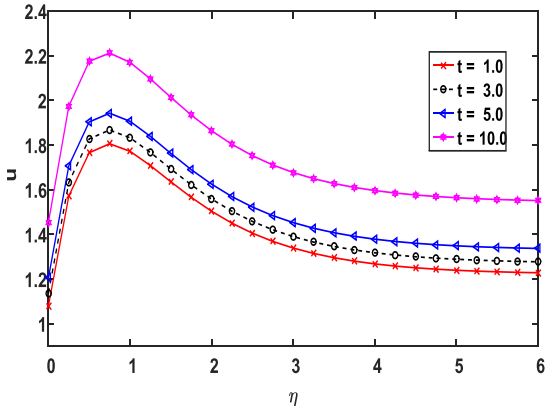

Figure 10: Velocity profiles against span wise co-ordinate η for different values of time t

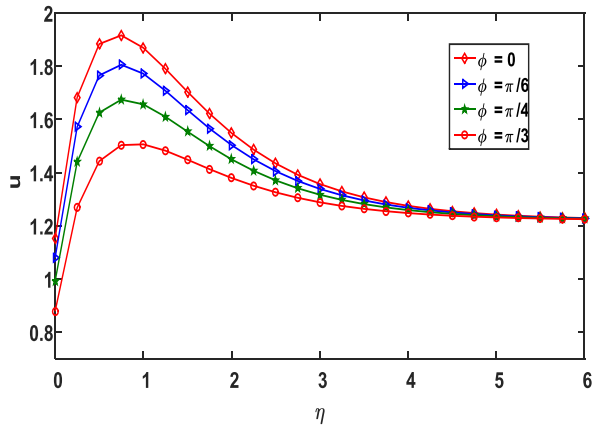

Figure 11: Velocity profiles against span wise co-ordinate η for different values of angle of inclinationϕ

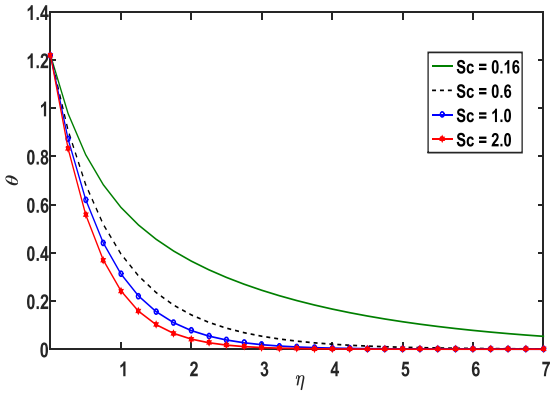

Figure12: Temperature profiles against span wise co-ordinate η for different values of Schmidt number Sc

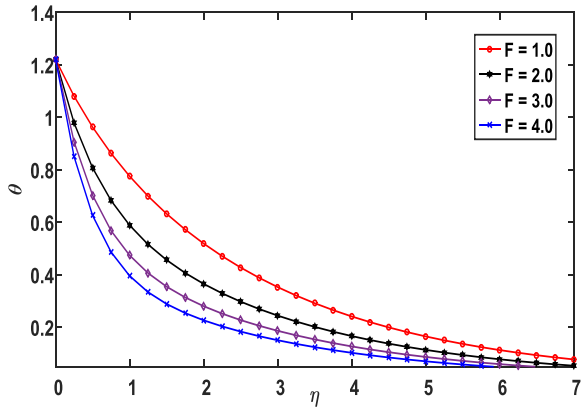

Figure13: Temperature profiles against span wise co-ordinate η for different values of radiation parameter F

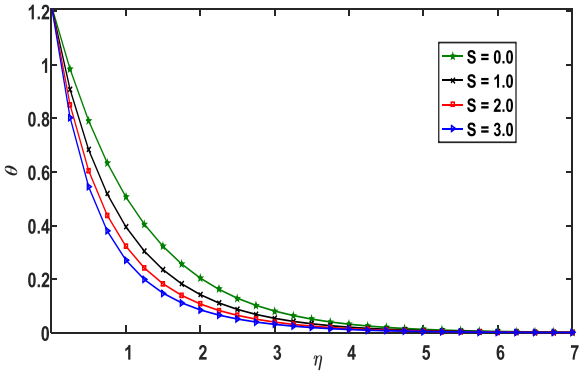

Figure14: Temperature profiles against span wise co-ordinate η for different values of heat absorption parameter S

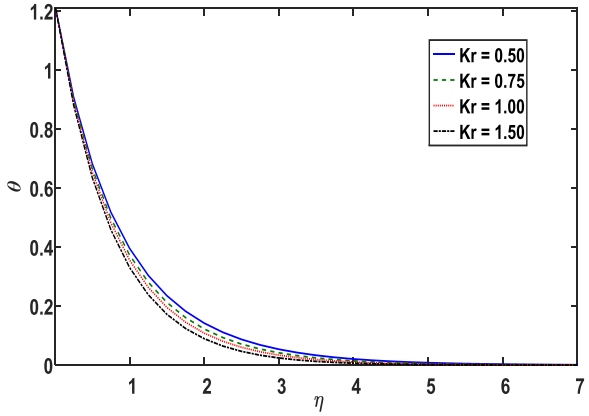

Figure15: Temperature profiles against span wise co-ordinate η for different values of chemical reaction parameter Kr

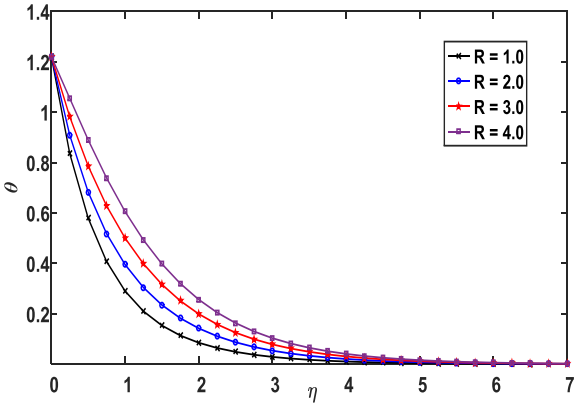

Figure16: Temperature profiles against span wise co-ordinate η for different values of absorption radiation parameter R

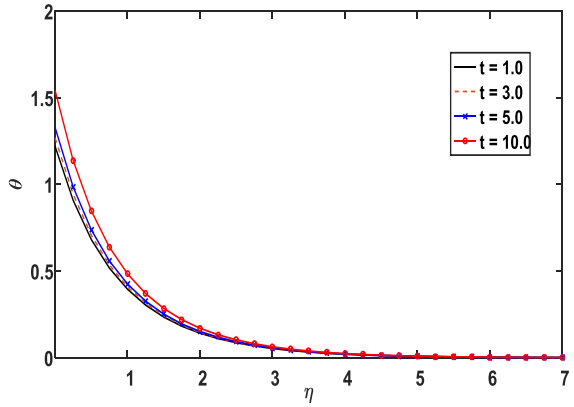

Figure 17: Temperature profiles against span wise co-ordinate η for different values of time t

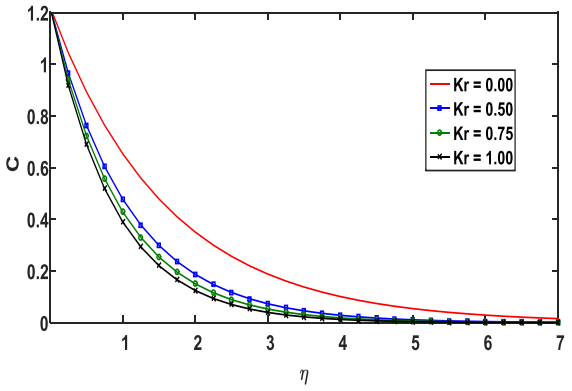

Figure 18: Concentration profiles against span wise co-ordinate η for different values of chemical reaction parameter Kr

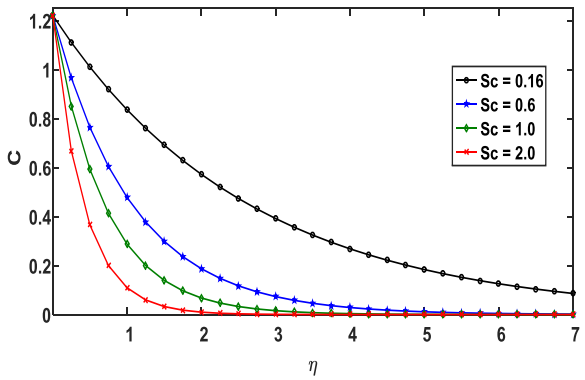

Figure 19: Concentration profiles against span wise co-ordinate η for different values of Schmidt number Sc

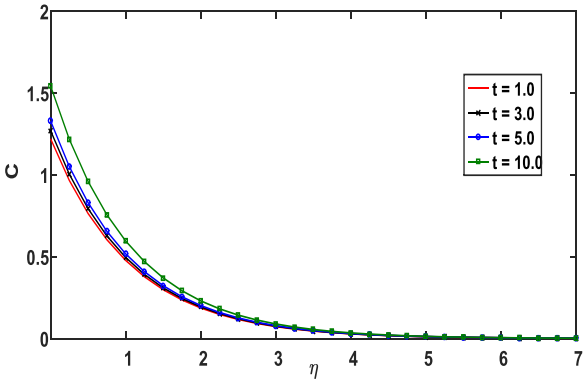

Figure 20: Concentration profiles against span wise co-ordinate η for different values of time t

Table 1: Skin-friction coefficient (Pr = 0.7, M = 2.0)

Sc	Kr	F	R	S	Gr	Gm	K_1	ϕ	C_f
0.16	**0.50**	**2**	**2**	**2**	**4**	**2**	**0.3**	**π/3**	**2.2645**
0.60	0.50	2	2	2	4	2	0.3	π/3	2.2109
1.00	0.50	2	2	2	4	2	0.3	π/3	2.1787
0.16	**0.75**	2	2	2	4	2	0.3	π/3	2.2573
0.16	**1.00**	2	2	2	4	2	0.3	π/3	2.2514
0.16	0.50	**1**	2	2	4	2	0.3	π/3	2.2879
0.16	0.50	**3**	2	2	4	2	0.3	π/3	2.2473
0.16	0.50	2	**1**	2	4	2	0.3	π/3	2.2334
0.16	0.50	2	**3**	2	4	2	0.3	π/3	2.2956
0.16	0.50	2	2	**1**	4	2	0.3	π/3	2.2879
0.16	0.50	1	2	**3**	4	2	0.3	π/3	2.2473
0.16	0.50	1	2	2	**2**	2	0.3	π/3	2.1106
0.16	0.50	1	2	2	**3**	2	0.3	π/3	2.1875
0.16	0.50	1	2	2	4	**1**	0.3	π/3	2.1702
0.16	0.50	1	2	2	4	**3**	0.3	π/3	2.3587
0.16	0.50	1	2	2	4	2	**0.1**	π/3	3.6485
0.16	0.50	1	2	2	4	2	**0.5**	π/3	1.7426
0.16	0.50	1	2	2	4	2	0.5	π/6	**2.7910**
0.16	0.50	1	2	2	4	2	0.5	π/4	**2.6033**

Table 2: Nusselt number

Sc	**F**	**S**	**R**	**Kr**	***Nu***
0.6	**2**	**1**	**2**	**0.5**	-1.4809
1.0	2	1	2	0.5	-1.6461
2.0	2	1	2	0.5	-1.8310
0.6	**3**	1	2	0.5	-1.8285
0.6	**4**	1	2	0.5	-2.1250
0.6	2	**2**	2	0.5	-1.8285
0.6	2	**3**	2	0.5	-2.1250
0.6	2	1	**3**	0.5	-1.0609
0.6	2	1	**4**	0.5	-0.6410
0.6	2	1	2	**1.0**	-1.5562
0.6	2	1	2	**1.5**	-1.6074

Table 3: Sherwood number

Sc	**Kr**	***Sh***
0.16	**0.5**	-0.4629
0.6	0.5	-1.1457
1.0	0.5	-1.7648
2.0	0.5	-2.9465
0.6	**0.75**	-1.2781
0.6	**1.0**	-1.3936
0.6	**1.5**	-1.5922

Table 4: Comparison of present results with those of Kim [12] with different values of M for C_f and N_u

Kim [12]			Present results $F = 0$, $S = 0$, $R = 0$, $K_1 = 0$, $Gm = 0$ and $\phi = 0$	
M	**C_f**	**Nu**	**C_f**	**Nu**
0.0	4.5383	-0.9430	4.5381	-0.9430
2.0	3.9234	-0.9430	3.9229	-0.9430
5.0	4.4457	-0.9430	4.4445	-0.9430
10.0	5.2976	-0.9430	5.2966	-0.9430

V. CONCLUSIONS

The theoretical solution of fluid flow past an inclined permeable surface in the presence of chemical reaction and thermal radiation has been studied. The dimensionless governing equations are solved by the perturbation technique. The effects of different parameters are studied graphically. The conclusions for this present fluid flow are given below:

- Velocity increases with the increase in absorption radiation parameter *R*, thermal Grashof number *Gr*, solutal Grashof number *Gm*, porous parameter K_1 and time *t*.
- Velocity decreases with increase in magnetic parameter *M*, radiation parameter *F*, chemical reaction parameter *Kr*, heat absorption parameter *S*, Schmidt number *Sc* and angle of inclination ϕ.
- The temperature decreases with the increase of Schmidt number *Sc*, chemical reaction parameter *Kr*, radiation parameter *F* and heat absorption parameter *S*.
- The temperature increases with increase of absorption radiation parameter *R* and time *t*.
- Concentration decreases with increase of Schmidt number *Sc* and chemical reaction parameter *Kr*.
- Concentration increase with increase of time *t*.
- The skin friction decreases with the increase of *Sc*, *Kr*, *F*, *S*, K_1 and ϕ and it increases with the increase of *R*, *Gr* and *Gm*.
- Nusselt number decreases with the increase of *Sc*, *F*, *S* and *Kr* and it falls with the rise in *R*.
- Sherwood number decreases with increase in chemical reaction parameter *Kr* or Schmidt number *Sc*.

APPENDIX

$$m_1 = \frac{Sc + \sqrt{Sc^2 + 4KrSc}}{2}, \qquad m_2 = \frac{Sc + \sqrt{Sc^2 + 4Sc(Kr + n)}}{2},$$

$$m_3 = \frac{\Pr + \sqrt{\Pr^2 + 4\Pr(F + S)}}{2}, \qquad m_4 = \frac{\Pr + \sqrt{\Pr^2 + 4\Pr(F + S + n)}}{2},$$

$$m_5 = \frac{1 + \sqrt{1 + 4M}}{2}, \qquad m_6 = \frac{1 + \sqrt{1 + 4(M + n)}}{2},$$

$$B_1 = \frac{AScm_1}{m_1^2 - m_1 - Sc(Kr + n)}, \qquad B_2 = 1 - B_1,$$

$$B_3 = \frac{-\Pr R}{m_1^2 - \Pr m_1 - \Pr(F + S)}, \qquad B_4 = 1 - B_3,$$

$$B_5 = \frac{\Pr Am_1 B_3 - \Pr RB_1}{m_1^2 - m_1 \Pr - \Pr(F + S + n)}, \qquad B_6 = \frac{-\Pr RB_2}{m_2^2 - m_2 \Pr - \Pr(F + S + n)},$$

$$B_7 = \frac{-\Pr RB_2}{m_2^2 - m_2 \Pr - \Pr(F + S + n)}, \qquad B_8 = 1 - B_5 - B_6 - B_7,$$

$$B_9 = \frac{-(Gr_1 B_3 + Gm_1)}{m_1^2 - m_1 - M}, \qquad B_{10} = \frac{-Gr_1 B_4}{m_3^2 - m_3 - M},$$

$$B_{11} = -\frac{(m_1 k_1 B_9 + m_3 k_1 B_{10} + B_9 + B_{10} + 1)}{!+ m_5 K_1},$$

$$B_{12} = \frac{Am_1 B_9 - Gr_1 B_5 - Gm_1 B_1}{m_1^2 - m_1 - (M + n)}, \qquad B_{13} = \frac{-Gr_1 B_6 - Gm_1 B_2}{m_2^2 - m_2 - (M + n)},$$

$$B_{14} = \frac{Am_3 B_{10} - Gr_1 B_7}{m_3^2 - m_3 - (M + n)}, \qquad B_{15} = \frac{-Gr_1 B_8}{m_4^2 - m_4 - (M + n)},$$

$$B_{16} = \frac{Am_5 B_{11}}{m_5^2 - m_5 - (M + n)},$$

$$B_{17} = \frac{-\left[B_{12}(1 + m_1 k_1) + B_{13}(1 + m_2 k_1) + B_{14}(1 + m_3 k_1) + B_{15}(1 + m_4 k_1) + B_{16}(1 + m_5 k_1) + 1\right]}{(1 + m_6 k_1)}$$

$Gr_1 = Gr\cos\phi$ and $Gm_1 = Gm\cos\phi$

REFERENCES

[1] Chen TS, Armaly BF, Mixed convection in external flow, In: KaKac S, Shah RK, Aung W, editors. Hand book of single-phase convective heat transfer. New York Wiley, 1987.

[2] Pop I, Ingham DB, Convective heat transfer, Mathematical and computational modeling of viscous fluids and porous media, Oxford: Pergamon Press; 2001.

[3] Soundalgekar VM, Gupta SK, Birajdar NS, Effects of mass transfer and free effects on MHD stokes problem for a vertical plate, Nucl Eng Res, 53, 309-406, 1979.

[4] Elbhasheshy EMA, Heat and mass transfer along a vertical plate surface tension and concentration in the presence of magnetic field, International Journal of Engineering Science, 34(5), 515-522, 1997.

[5] Hossain MA, Taklhar MS, Radiation effect on mixed convection along a vertical plate with uniform surface temperature, Heat and Mass Transfer, 31, 243-248, 1996.

[6] Aboeldahab Emad M. Radiation effect on heat transfer in electrically conducting fluid at a stretching surface with uniform free stream, Journal of Physics D Applied Physics, 33, 3180-3185, 2000.

[7] Muthucumarswamy R, Kumar Senthil G, Heat and mass transfer effects on moving vertical plate in the presence of thermal radiation, Theoretical Applied Mechanics, 31, 35-46, 2004.

[8] Abo-Eldahad EM, Elgendy MS, Radiation effect on convective heat transfer in an electrically conducting fluid at a stretching surface with variable viscosity and uniform free stream, Physics Scr, 62, 321-325, 2000.

[9] Seddeek MA, Effects of radiation and variable viscosity on a MHD free convection past a semi-infinite flat plate with an aligned magnetic field in the case of unsteady flow, International Journal of Heat and Mass Transfer, 45, 931-935, 2002.

[10] Abdus Satter MD, Hamid Kalim MD, Unsteady free convection interaction with thermal radiation in a boundary layer flow past a vertical porous plate, Journal of Math Phys. Sci. 30, 25-37, 1996.

[11] Cortell R. Effects of viscous dissipation and radiation on the thermal boundary layer flow over a non-linearly stretching sheet, Physics Letter, A372(5), 631-636, 2008.

[12] Kim YJ. Unsteady MHD convective heat transfer past a semi-infinite vertical porous moving plate with variable suction, International Journal of Engineering Science, 38, 833-845, 2000.

[13] Nield D, Bejan A. Convection in porous media. New York: Springer, 1999.

[14] Cheng P. Heat transfer in geothermal system, Adv Heat Transfer, 14, 1-105, 1978.

[15] Rudraiah N, Flow through and past porous media, Encyclopedia of fluid mechanics, Gulf Publ 5, 567-647, 1986.

[16] Beavers GS, Joseph DD. Boundary conditions at a naturally permeable wall, Journal of Fluid Mechanics, 30, 197-207, 1967.

[17] Saffman PG, on the boundary conditions at the surface of a porous medium. Stud Appl. Math, 1, 93-101, 1971.

[18] Nield DA, Onset of convection in a fluid layer overlying a layer of porous medium, Journal of Fluid Mechanics, 81, 513-522, 1967.

[19] Nield DA, Boundary correction for the Rayleigh-Darcy problem, limitations of the Brinkman equation, Journal of Fluid Mechanics, 128, 37-46, 1983.

[20] Poulikakos D, Bejan A, Selimos B, Blake KR, High Rayleigh number convection in a fluid overlying a porous bed, International Journal of Heat Fluid flow, 7, 109-114, 1986.

[21] Rudraiah N, Dulal Pal, Shiva Kumar PN, Effect of slip and magnetic field on composite system, Fluid Dynamics Research, 4, 255-270, 1988.

[22] Umemura, A. and Law, C. K, Natural convection boundary layer flow over a heated plate with arbitrary inclination, J. Fluid Mech., 219, 571-584, 1990.

[23] Hossain, M. A. Pop, I. and Ahamad, M, MHD free convection flow from an isothermal plate inclined at a small angle to the horizontal, J. Theo. Appl. Fluid Mech., 1,194-207, 1996.

[24] Anghel, M. Hossain, M. A. Zeb, S. and Pop, I. Combined heat and mass transfer by free convection past an inclined flat plate, Int. J. Appl. Mech. and Engg., 2, 473-497, 2001.

[25] Chen, C. H.Heat and mass transfer in MHD flow by natural convection from a permeable inclined surface with variable wall temperature and concentration, Acta Mechanica., 172, 219- 235, 2004.

[26] Sivasankaran, S. Bhuvaneswari, M. Kandaswamy, P. and Ramasami, E. K. Lie Group Analysis of Natural Convection Heat and Mass Transfer in an Inclined Surface, Non-linear Analysis; Modeling and Control., Vol. II (l), 201- 212, 2006.

[27] Bhuvaneswari,M. Sivasankaran, S. and Kim, Y J. Exact analysis of radiation convective flow heat and mass transfer over an inclined plate in a porous medium, World Applied Sciences Journal.10, 774-778, 2010.

[28] Jyothi Bala, A. and Vijaya Kumar Varma, S. Unsteady MHD heat and mass transfer flow past a semi-infinite vertical porous moving plate with variable suction in the presence of heat generation and homogeneous chemical reaction, Int. J. of Appl. Math and Mech. 7 (7). 20-44, 2011.
[29] Hitesh Kumar, An analytical solution to the problem of radiative heat and mass transfer over an inclined plate at prescribed heat flux with chemical reaction, J. Serb. Chem. Soc. 77, 1-14, 2012.
[30] Mastharao S, Balamurugan KS and Varma SVK, Chemical reaction effects on MHD free convection flow through a porous medium bounded by an inclined surface, International Journal of Mathematics and Computer Applications Research, 3(3), 13-22, 2013.

Y. Satheesh Kumar Reddy "Unsteady Magnetohyrdro Dynamic Convective Heat and Mass Transfer in a Boundary Layer Slip Flow past an Inclined Permeable Surface In The Presence Of Chemical Reaction and Thermal Radiation" International Refereed Journal of Engineering and Science (IRJES), vol. 07, no. 02, 2018, pp. 16–29.